low-density particles include spheres with silicate cores and organic mantles, carbonaceous spheres, or aggregates of these. Of the seven candidate ISD particles, one is plausibly dominated by carbon and one is primarily a single silicate with a mantle-core structure, whereas the others are complex aggregates of various micrometer- to nanometer-size phases such as oxides, metal, and sulfides, in addition to silicate (Table 1).

The need for internal consistency leaves us with a twofold conclusion: If large interstellar dust particles consist of compact silicates with optical properties similar to those assumed by Landgraf *et al.* (*4*), then our results are in conflict with the U/G observations, and consistent with astronomical observations (*45*). By contrast, if large interstellar dust particles have low densities, which appears to be more likely based on trajectories, capture speeds, and compositions of our candidates, then our data can be consistent with the U/G observations, and possibly also with the astronomical observations, depending on the (currently unknown) wavelength dependence of the extinction cross sections of these particles. The latter conclusion is encouraging news for any future sample-return missions with the goal of capturing large numbers of relatively intact interstellar dust particles.

## REFERENCES AND NOTES


1. P. C. Frisch, J. D. Slavin, *Earth Planets Space* **65**, 175–182 (2013).
2. H. Kimura, I. Mann, E. K. Jessberger, *Astrophys. J.* **583**, 314–321 (2003).
3. B. T. Draine, *Annu. Rev. Astron. Astrophys.* **41**, 241–289 (2003).
4. M. Landgraf, W. J. Baggaley, E. Grun, H. Kruger, G. Linkert, *J. Geophys. Res. Space Phys.* **105**, 10343–10352 (2000).
5. E. Grün *et al.*, *Nature* **362**, 428–430 (1993).
6. H. Krüger *et al.*, *Planet. Space Sci.* **58**, 951–964 (2010).
7. All particle sizes heareafter are given in diameter, rather than radius.
8. D. Brownlee *et al.*, *Science* **314**, 1711–1716 (2006).
9. A. J. Westphal *et al.*, *Meteorit. Planet. Sci.* 10.1111/maps.12168 (2014).
10. D. R. Frank *et al.*, *Meteorit. Planet. Sci.* 10.1111/maps.12147 (2014).
11. H. A. Bechtel *et al.*, *Meteorit. Planet. Sci.* 10.1111/maps.12125 (2014).
12. A. L. Butterworth *et al.*, *Meteorit. Planet. Sci.* 10.1111/maps.12220 (2014).
13. F. E. Brenker *et al.*, *Meteorit. Planet. Sci.* 10.1111/maps.12206 (2014).
14. A. S. Simionovici *et al.*, *Meteorit. Planet. Sci.* 10.1111/maps.12208 (2014).
15. G. J. Flynn *et al.*, *Meteorit. Planet. Sci.* 10.1111/maps.12144 (2014).
16. Z. Gainsforth *et al.*, *Meteorit. Planet. Sci.* 10.1111/maps.12148 (2014).
17. F. Postberg *et al.*, *Meteorit. Planet. Sci.* 10.1111/maps.12173 (2014).
18. V. J. Sterken *et al.*, *Meteorit. Planet. Sci.* 10.1111/maps.12219 (2014).
19. R. M. Stroud *et al.*, *Meteorit. Planet. Sci.* 10.1111/maps.12136 (2014).
20. A. J. Westphal *et al.*, *Meteorit. Planet. Sci.* 10.1111/maps.12221 (2014).
21. Supplementary details are available on *Science* Online.
22. R. Lallement, J. L. Bertaux, *Astron. Astrophys.* **565**, A41 (2014).
23. M. C. Price *et al.*, *Meteorit. Planet. Sci.* **45**, 1409–1428 (2010).
24. M. C. Price *et al.*, *Meteorit. Planet. Sci.* **47**, 684–695 (2012).
25. A. T. Kearsley *et al.*, *Meteorit. Planet. Sci.* **43**, 41–73 (2008).
26. A. J. Westphal *et al.*, *Meteorit. Planet. Sci.* **39**, 1375–1386 (2004).
27. P. Tsou, D. E. Brownlee, S. A. Sandford, F. Horz, M. E. Zolensky, *J. Geophys. Res. Planets* **108**, 8113 (2003).
28. S. A. Sandford *et al.*, *Meteorit. Planet. Sci.* **45**, 406–433 (2010).
29. J. P. Bradley, *Science* **265**, 925–929 (1994).
30. L. P. Keller, S. Messenger, *Geochim. Cosmochim. Acta* **75**, 5336–5365 (2011).
31. P. C. Frisch *et al.*, *Science* **341**, 1080–1082 (2013).
32. V. Dikarev, E. Grün, M. Landgraf, W. J. Baggaley, D. P. Galligan, in *Proceedings of the Meteoroids 2001 Conference*, B. Warmbein, Ed. (2001), vol. 495, pp. 609–615.
33. M. Landgraf, M. Müller, E. Grün, *Planet. Space Sci.* **47**, 1029–1050 (1999).
34. M. J. Burchell, M. J. Cole, M. C. Price, A. T. Kearsley, *Meteorit. Planet. Sci.* **47**, 671–683 (2012).
35. N. Gehrels, *Astrophys. J.* **303**, 336–346 (1986).
36. H. Krüger, E. Grün, *Space Sci. Rev.* **143**, 347–356 (2009).
37. M. Min, J. W. Hovenier, L. B. F. M. Waters, A. de Koter, *Astron. Astrophys.* **489**, 135–141 (2008).
38. E. B. Jenkins, *Astrophys. J.* **700**, 1299–1348 (2009).
39. F. Kemper, W. J. Vriend, A. G. G. M. Tielens, *Astrophys. J.* **609**, 826–837 (2004).
40. F. Kemper, W. J. Vriend, A. Tielens, *Astrophys. J.* **633**, 534–534 (2005).
41. A. P. Jones, J. A. Nuth III, *Astron. Astrophys.* **530**, A44 (2011).
42. F. J. Molster, L. Waters, *Astromineralogy* **609**, 121–170 (2003).
43. S. Messenger, L. P. Keller, D. S. Lauretta, *Science* **309**, 737–741 (2005).
44. C. Vollmer, P. Hoppe, F. E. Brenker, C. Holzapfel, *Astrophys. J.* **666**, L49–L52 (2007).
45. B. T. Draine, *Space Sci. Rev.* **143**, 333–345 (2009).


## ACKNOWLEDGMENTS


We are deeply grateful to the Stardust@home dusters (list at http://stardustathome.ssl.berkeley.edu/sciencedusters), whose tremendous efforts were critically important to the success of this project. The ISPE consortium gratefully acknowledges the NASA Discovery Program for Stardust, the fourth NASA Discovery mission. NASA grants supported the following authors: NNX09AC36G—A.J.W., A.L.B., Z.G., R.L., D.Z., W.M., and J.V.K.; NNX09AC63G—C.F., R.D., A.L., W.J.O., K.S., and F.J.S.; NNH11AQ61I—R.M.S., H.C.G., and N.D.B.; NNX11AC21G—A.M.D., A.J.K., and T.S.; NNX11AE15G—G.J.F. The Advanced Light Source and the National Center for Electron Microscopy are supported by the Director, Office of Science, Office of Basic Energy Sciences, of the U.S. Department of Energy (DOE) under contract no. DE-AC02-05CH11231. Use of the National Synchrotron Light Source, Brookhaven National Laboratory, was supported by the U.S. DOE, Office of Science, Office of Basic Energy Sciences, under contract no. DE-AC02-98CH10886. Use of the Advanced Photon Source, an Office of Science User Facility operated for the U.S. DOE Office of Science by Argonne National Laboratory, was supported by the U.S. DOE under contract no. DE-AC02-06CH11357. M.T. and F.P. acknowledge support by Klaus Tschira foundation. A.A. and P.R.H. were supported by the Tawani Foundation. M.J.B. and M.C.P. are supported by Science and Technology Facilities Council (UK). F.E.B., J.K.H., P.H., J.L., F.P., S.S., R.S., and M.T. were supported by funding of the German Science Foundation (DFG) within SPP1385: the first ten million years of the solar system—a planetary materials approach. The ESRF ID13 measurements were performed in the framework of ESRF LTP EC337, with financial support by the Funds for Scientific Research (FWO), Flanders, Belgium (contract nr. G.0395.11, G.0257.12N and Big Science program G.0C12.13). G. Silversmit was postdoctoral fellow of the FWO during the ISPE investigations. Data presented in this paper are described in the supplementary materials and in references (*9*–*20*).


## SUPPLEMENTARY MATERIALS

www.sciencemag.org/content/345/6198/786/suppl/DC1
Materials and Methods
Supplementary Text
Figs. S1 to S8
Tables S1 to S3
References (*46*–*56*)


21 February 2014; accepted 9 July 2014
10.1126/science.1252496


REPORTS

INTERSTELLAR MEDIUM

# Pseudo–three-dimensional maps of the diffuse interstellar band at 862 nm


**Janez Kos,[1]* Tomaž Zwitter,[1] Rosemary Wyse,[2] Olivier Bienaymé,[3] James Binney,[4] Joss Bland-Hawthorn,[5] Kenneth Freeman,[6] Brad K. Gibson,[7] Gerry Gilmore,[8] Eva K. Grebel,[9] Amina Helmi,[10] Georges Kordopatis,[8] Ulisse Munari,[11] Julio Navarro,[12] Quentin Parker,[13,14,15] Warren A. Reid,[13,14] George Seabroke,[16] Sanjib Sharma,[5] Arnaud Siebert,[3] Alessandro Siviero,[17,18] Matthias Steinmetz,[18] Fred G. Watson,[15] Mary E. K. Williams[18]**



**The diffuse interstellar bands (DIBs) are absorption lines observed in visual and near-infrared spectra of stars. Understanding their origin in the interstellar medium is one of the oldest problems in astronomical spectroscopy, as DIBs have been known since 1922. In a completely new approach to understanding DIBs, we combined information from nearly 500,000 stellar spectra obtained by the massive spectroscopic survey RAVE (Radial Velocity Experiment) to produce the first pseudo–three-dimensional map of the strength of the DIB at 8620 angstroms covering the nearest 3 kiloparsecs from the Sun, and show that it follows our independently constructed spatial distribution of extinction by interstellar dust along the Galactic plane. Despite having a similar distribution in the Galactic plane, the DIB 8620 carrier has a significantly larger vertical scale height than the dust. Even if one DIB may not represent the general DIB population, our observations outline the future direction of DIB research.**


Diffuse instellar bands (DIBs) are wide and sometimes structured absorption lines in the optical and near-infrared (NIR) wavelengths that originate in the interstellar medium (ISM) and were discovered in 1922 (*1*, *2*); more than 400 are known today (*3*), but their physical carriers are still unidentified (*4*–*8*). Their abundances are correlated with interstellar extinction and with abundances of some simple molecules (*9*), so DIBs are probably

associated with carbon-based molecules (*2*). DIBs show no polarization effects (*1*) and are likely positively charged (*10*), as suggested by the relatively low energies of absorbed photons (*11*). No known transition of any molecule or atom has yet been found to match the central wavelengths of the DIBs (*2*). Their origin and chemistry are thus unknown, a unique situation given the distinctive family of many absorption lines within a limited spectral range. Like most molecules in the ISM that have an interlaced chemistry, DIBs may play an important role in the life-cycle of the ISM species and are the last step to fully understanding the basic components of the ISM. The problem of their identity is more intriguing given the possibility that the DIB carriers are organic molecules. DIBs remain a puzzle for astronomers studying the ISM, physicists interested in molecular spectra, and chemists studying possible carriers in the laboratories.

The maps presented here are based on data from the recently completed RAVE (Radial Velocity Experiment) spectroscopic survey (*12*) and are limited to one DIB. However, extensive surveys of Galactic stars (*13*–*17*) that are starting now will permit spatial mapping, the study of environmental constraints, and a comparison of the spatial distribution for over a dozen DIBs, interstellar molecules, and dust with techniques similar to the ones described here. Large spectroscopic surveys observing ~$10^5$ stars are a big leap forward from previous DIB-specific surveys, in which only a few thousand stars were observed at most (*18*, *19*), or only around a hundred stars, if weaker DIBs were observed (*20*).

Making a three-dimensional (3D) map of an ISM species from absorption lines in stellar spectra is a challenge, requiring a large number of observed lines of sight with measured abundances of the ISM species, as well as the distances to the observed stars. The DIB carrier can be found anywhere along the line of sight to the observed star, so the distance to the DIB carrier is uncertain, with only an upper limit from the distance to the star. It can only be established through the observations of many stars within a small solid angle but at different distances. To produce a map, such sets of observations must be achievable in any direction. The RAVE survey fulfills these requirements. In the pre-Gaia era, we have precise distances only to Hipparcos stars and a few others. For maps to be made at distances larger than the Hipparcos sample, spatial resolution must be sacrificed, as the distance measurements are less precise and errors in distance calculations will exceed the typical size of the ISM clumps.

DIBs are more numerous than absorption lines of other ISM species in the optical and NIR bands and are therefore ideal to be studied in general spectroscopic surveys, as they are present in almost any band observed by the surveys mentioned above. Having observations of multiple DIBs also allows the study of different parameters (*21*) of the ISM apart from observing the spatial distribution of a single species.

DIBs are traditionally observed in the spectra of hot stars, where interstellar lines rarely blend with stellar ones, but hot stars are intrinsically rare. With new analytical methods (*22*, *23*), it is possible to observe DIBs in the spectra of cool stars, which dominate in most spectroscopic surveys. In the (magnitude-limited) RAVE survey, only 1.1% of the stars have effective temperature above 8000 K. Our method makes use of a large database of RAVE spectra and requires neither knowledge of stellar parameters nor the use of synthetic spectra (*22*). For each spectrum, a number of most-similar stellar spectra were

[1]Faculty of Mathematics and Physics, University of Ljubljana, Jadranska 19, 1000 Ljubljana, Slovenia. [2]Johns Hopkins University, Homewood Campus, 3400 North Charles Street, Baltimore, MD 21218, USA. [3]Observatoire astronomique de Strasbourg, Université de Strasbourg, CNRS, 11 rue de l'Université, F-67000 Strasbourg, France. [4]Rudolf Peierls Centre for Theoretical Physics, Keble Road, Oxford OX1 3NP, UK. [5]Sydney Institute for Astronomy, School of Physics A28, University of Sydney, NSW 2008, Australia. [6]Research School of Astronomy and Astrophysics, Australian National University, Canberra, Australia. [7]Chair, Computational Astrophysics, Jeremiah Horrocks Institute, University of Central Lancashire, Preston PR1 2HE, UK. [9]Institute of Astronomy, Madingley Road, Cambridge CB3 0HA, UK. [9]Astronomisches Rechen-Institut, Zentrum für Astronomie der Universität Heidelberg, Mönchhofstraße 12–14, D-69120 Heidelberg, Germany. [10]Kapteyn Astronomical Institute, Post Office Box 800, NL-9700 AV Groningen, Netherlands. [11]Instituto Nazionale di Astrofisica Astronomical Observatory of Padova, 36012 Asiago (VI), Italy. [12]University of Victoria, Victoria BC, Canada V8P 5C2. [13]Department of Physics and Astronomy, Macquarie University, Sydney, NSW 2109, Australia. [14]Centre for Astronomy, Astrophysics and Astrophotonics, Macquarie University, Sydney, NSW 2109, Australia. [15]Australian Astronomical Observatory, Post Office Box 915, North Ryde, NSW 1670, Australia. [16]Mullard Space Science Laboratory, University College London, Holmbury St Mary, Dorking RH5 6NT, UK. [17]Department of Physics and Astronomy, Padova University, Vicolo dell'Osservatorio 2, I-35122 Padova, Italy. [18]Leibniz-Institut für Astrophysik Potsdam (AIP), An der Sternwarte 16, 14482 Potsdam, Germany.
***Corresponding author. E-mail: janez.kos@fmf.uni-lj.si**

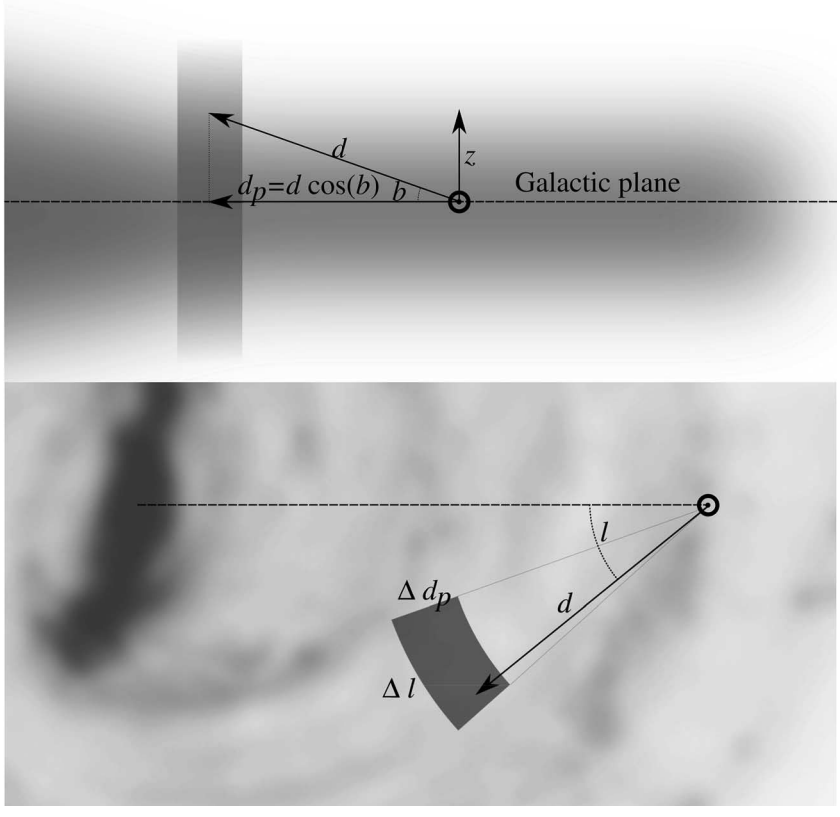


**Fig. 1. Coordinate system for spatial sampling of the DIB carrier and dust in the Galaxy. Top:** Side-view of two columns, representing two bins (one stretching from the Galactic plane in the positive *z* direction and one in the negative *z* direction), giving two data points, one for each Galactic hemisphere. The height of the column above (or below) the Galactic plane is limited to 1.5 kpc in *z* and 40° in Galactic latitude, primarily to avoid using any spectra that were normalized by a large factor, as the normalization enhances the noise. Because most of the gas and dust is located near the Galactic plane, this limitation should not influence the final results. **Bottom:** Face-on view of one column, representing one bin, giving one data point. The columns are segments of equally spaced cylindrical shells. In the first shell, there are three columns, and in each following shell there are $3(2n - 1)$ columns, where *n* is the number of the shell. All the columns thus have the same area of the cross-section and are as close to square as possible. To calculate the maps with different spatial resolutions, only the width of the shell is changed. *d* is the distance to a star, $d_p$ is the distance projected onto the Galactic plane, *b* and *l* are the Galactic latitude and longitude.

found in regions with very low extinction at high Galactic latitudes. From these spectra, we generated a stellar template to divide out the stellar contribution in the target spectrum. This leaves only the interstellar features in the spectrum: in this case, only the DIB at 862 nm. A detailed description of the DIB extraction method can be found in (*22*), which also shows that the RAVE data satisfy the prerequisities for the analysis of this paper: The DIB 8620 can be detected after the combination of several RAVE spectra; it can be detected at high Galactic latitudes; and the DIB strength correlates with the interstellar extinction. The DIB in (*22*) is measured more precisely than the extinction, as is reflected in the correlation plots.

Distances and extinctions are calculated jointly by a Bayesian algorithm (*24*). As input it takes photometric data and spectroscopic parameters of stellar atmospheres measured in RAVE survey, and it assumes asymptotic values of extinction from the SFD maps (*25*), corrected accordingly to known deviations. The value of the total V-band extinction, $A_V$, is the calculated parameter. [See (*26*) for a more detailed description.]

The number of observed stars in the RAVE proved to be high enough for this study only in the nearest 3 kpc of the Galaxy (*26*). The signal-to-noise (S/N) ratio of an individual RAVE spectrum is too low (the mode of the S/N values is 25) to detect the DIB in the spectrum of an individual star, so several spectra were combined to achieve a S/N ratio of ~300. The DIB is generally detectable in these combined spectra, and its strength can be measured with a precision of 10 to 20% [for details on combining spectra, see (*22*)]. This requirement to combine spectra is the limiting factor in the achievable spatial resolution. The resolution of a true 3D map would be low, so we produced a pseudo-3D map, where the distribution of the carrier in the $z$ direction (perpendicular to the Galactic plane) is described by an exponential law with a fixed scale height and a variable in-plane scaling factor, represented by a 2D map separately for the northern and the southern Galactic hemisphere (Fig. 1). Because of the highly variable star density in different volumes, the final maps vary in spatial resolution, between 75 and 400 pc. This allowed us to cover a wider volume of the Galaxy than we could with a better, but fixed, resolution. Combining spectra in a given bin also improved the distance value of each bin: Distance errors of 25% for individual stars are reduced when averaging over all stars in a bin, so that the error on the bin distance becomes smaller than the bin size.

An exponential law is a good approximation of the spatial distribution of the interstellar dust, as well as the strength of the DIB at 862 nm in the direction perpendicular to the Galactic plane (Fig. 2). The scale heights of the DIB and dust components differ significantly: 117.7 ± 4.7 pc

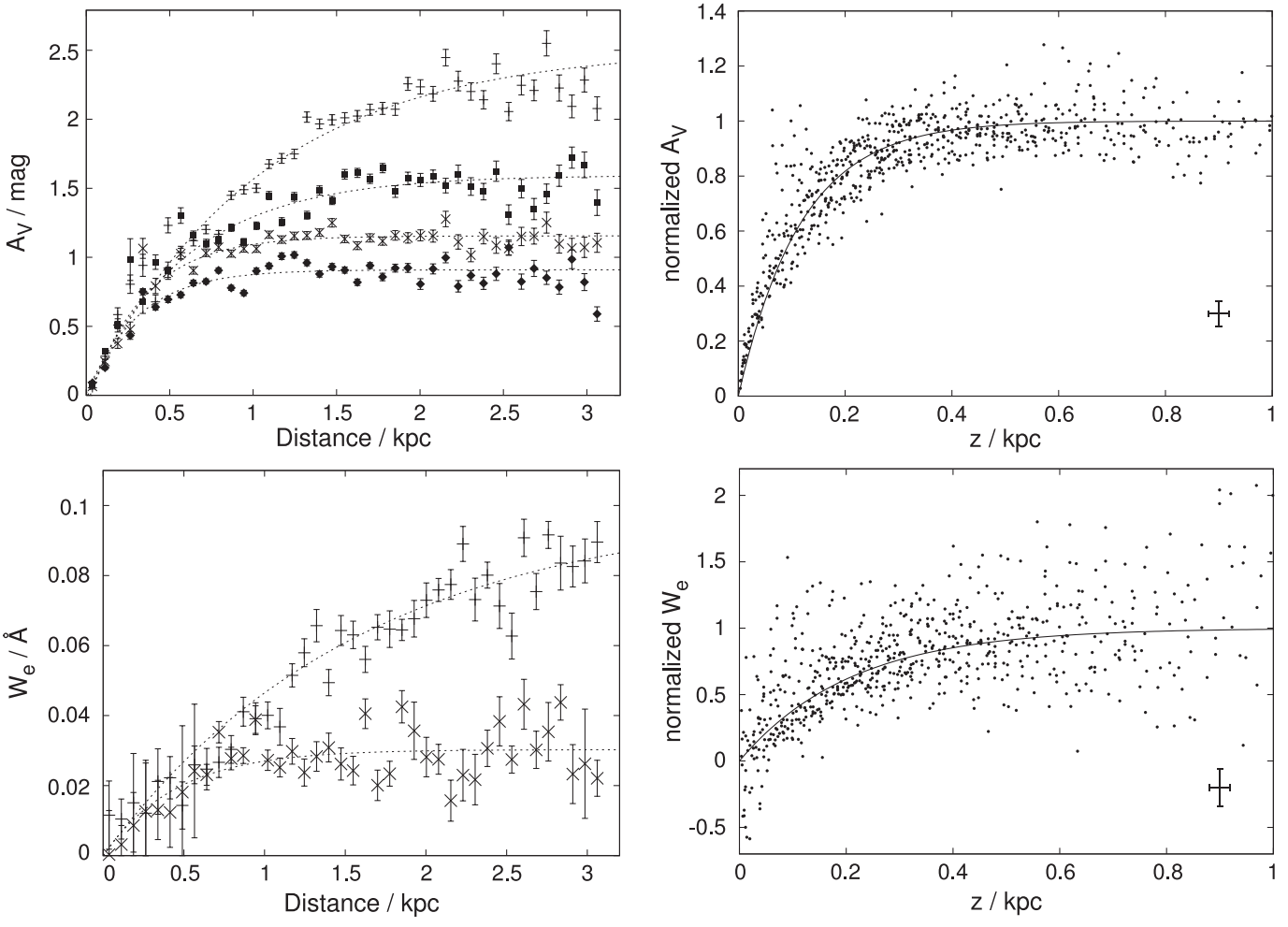


**Fig. 2. Determination of the scale height perpendicular to the Galactic plane.** The average extinction ($A_V$) was calculated by a Bayesian algorithm [top left (*26*)] and equivalent width ($W_e$) of the DIB (bottom left) of stars in 2° wide regions at different central Galactic latitudes ($b$) are shown as a function of distance. The averages extend over all longitudes in every region. Only four examples for the extinction (top to bottom: $b$ = −6°, $b$ = −10°, $b$ = −14°, $b$ = −18°) and two for the DIB (top to bottom: $b$ = −6°, $b$ = −14°) out of 20 regions are plotted here. Dashed curves are fitted exponential models. Data points from all 20 regions are represented in the same plot for the extinction (top right) and for the DIB (bottom right). Instead of the distances $d$, the distance from the Galactic plane $z = d \sin(|b|)$ was used, and each was normalized to unity to make the data at all Galactic latitudes comparable. The solid line is the fitted exponential model. Error bars in the bottom right corner represent a typical error of the data points.

for the dust and 209.0 ± 11.9 pc for the DIB-bearing gas. These two scale heights were used as constants uniformly through the whole region of the Galaxy included in this study. Some of the gas components, such as $H_2$ or CO (87 pc) (*27*, *28*) and probably Na I (<200 pc) (*29*), are consistent with the vertical distribution of the dust layer that we find, while a larger thickness of the DIB layer is similar to the one of Ca II (>200 pc) (*29*). H I has a profile of many components with an average half width at half maximum of 115 pc and large fluctuations (*30*). Massive stars, with a high ultraviolet luminosity, have a scale height even smaller than dust (*31*).

The strength of the DIB is measured as its equivalent width. The projected equivalent width has been normalized by an exponential law (*26*) and represents the equivalent width that would be measured if both the observer and the star were in the Galactic plane. The resulting maps show some distinctive features (Fig. 3). Most notable are large, narrow cavities, where the column density is low. In between these underdense regions lie clouds of the ISM, some with gentle increases in column density and some with well-defined boundaries. The smoother transitions are probably due to several less prominent clouds at different Galactic latitudes that collectively produce a gradient in that direction. We could recognize some known absorbing clouds (*26*), but the identification of other features is more difficult, as all the information in the $z$ direction is condensed into two data points, one for each hemisphere. Although spiral arms are elusive, a steeper rise in density is observed toward the longitudes between 320° and 60°, toward the Sagittarius arm and the Orion spur. We note that the projected equivalent width can decrease with distance. Different bins can represent stars at different Galactic latitudes, and the stars included in one bin can have more ISM in front of them than stars included in a more distant bin at the same Galactic longitude. However, the general rise that we find in the DIB equivalent width with distance increases confidence in the maps.

Because this work only studies one DIB, the detailed results should not be generalized to other DIBs. It is known, from other studies, that different DIBs show different behavior. The main difference that is expected among other DIBs is in the value of the vertical scale height and not so much in the projected equivalent width, because the former has little influence on the quite good correlation between DIBs and the interstellar extinction.

The projected distribution of the DIB-bearing gas (Fig. 3) is the first plot of its kind, as it is the

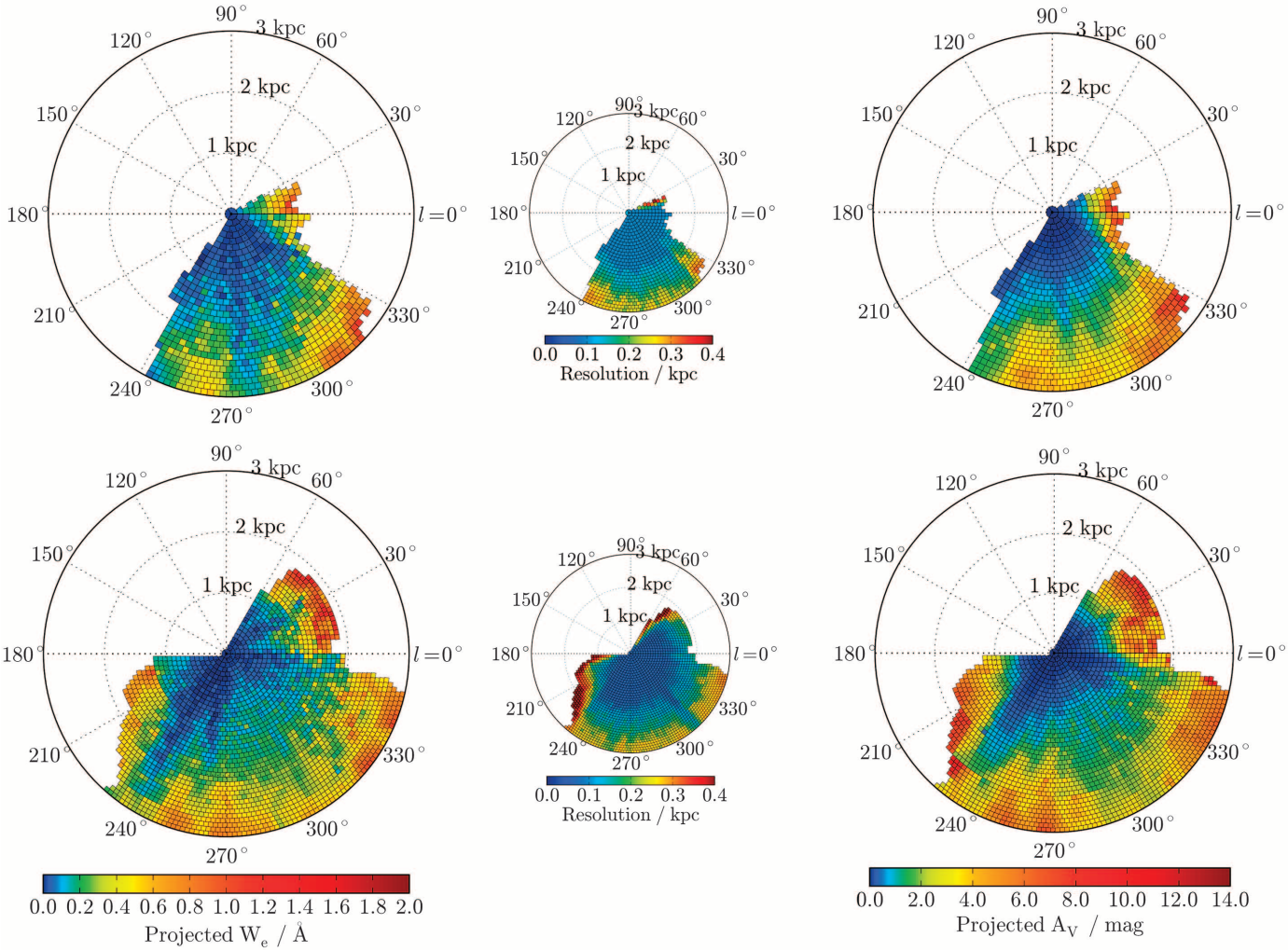


**Fig. 3. Projected equivalent width of the DIB at 862 nm, projected extinction, and the corresponding spatial resolution of the map.** The large maps show a color-coded projected equivalent width (left) and projected extinction (right). The small maps show the spatial resolution. Top and bottom three maps correspond to the northern and to the southern Galactic hemisphere, respectively. Notice the nonlinear color scale. Individual maps with spatial resolution between 0.8 and 0.075 kpc were used to make this combined result (*26*). The Sun is in the center of each map, with projected polar coordinates of the Galactic plane distance and the Galactic longitude. The stars analyzed in this study are located south of the celestial equator, which is why Galactic longitude and distance are incompletely sampled between the $l$ ~ 0° and $l$~ 210°. There are 1292 bins on the maps for the northern and 2212 bins on the maps for the southern Galactic hemisphere. The typical relative error of the extinction value in each bin is 14% and the relative error for the $W_e$ is 12%.

only map of any DIB carrier at this scale and the only one taking the distance information as a major parameter. Together with the measured scale height, this is the first 3D study of the spatial distribution of the DIB-bearing ISM clouds. The projected distribution of the extinction due to the interstellar dust is markedly similar to that of the DIB carrier [see (*26*) for the correlation analysis], confirming the strong correspondence between the two (*32*). The map of the extinction is itself an advance, as it maps the regions out of the Galactic plane and probes dust to greater distances than present maps (*33*) of these regions and is consistent with maps in the literature. Our success in producing the maps of the DIB carrier implies good prospects for future spectroscopic surveys (*14*–*16*) that will produce similar (*15*) or better quality (*14*, *16*) spectra and will also rely on DIBs to provide information about the ISM. Our work opens new possibilities in the study of DIBs and also offers a unique way of comparing DIBs with other interstellar species by studying their out-of-plane distribution. This can be translated into the study of physical and chemical properties of DIB carriers in the near future.

The measured 3D distribution, especially the unexpectedly high scale-height of the DIB 8620 carrier, calls for a theoretical explanation. There are two options—either the DIB carriers migrate to their observed distances from the Galactic plane, or they are created at these large distances, from components of the ISM having a similar distribution. The latter is simpler to discuss, as it does not require knowledge of the chemistry of the DIB carrier or processes in which the carriers are involved. Khoperskov and Shchekinov (*34*) showed that mechanisms responsible for dust migration to high altitudes above the Galactic plane segregate small dust particles from large ones, so the small ones form a thicker disk. This is also consistent with the observations of the extinction and reddening at high Galactic latitudes (*35*).

## REFERENCES AND NOTES


1. G. H. Herbig, *Annu. Rev. Astron. Astrophys.* **33**, 19–73 (1995).
2. P. J. Sarre, *J. Mol. Spectrosc.* **238**, 1–10 (2006).
3. L. M. Hobbs *et al.*, *Astrophys. J.* **705**, 32–45 (2009).
4. G. Galazutdinov, B.-C. Lee, I.-O. Song, M. Kazmierczak, J. Krełowski, *Mon. Not. R. Astron. Soc.* **412**, 1259 (2011).
5. J. Krełowski *et al.*, *Astrophys. J.* **714**, L64 (2010).
6. F. Salama, G. A. Galazutdinov, J. Krełowski, L. J. Allamandola, F. A. Musaev, *Astrophys. J.* **526**, 265–273 (1999).
7. S. Iglesias-Groth *et al.*, *Mon. Not. R. Astron. Soc.* **407**, 2157–2165 (2010).
8. J. P. Maier *et al.*, *Astrophys. J.* **726**, 41 (2011).
9. J. A. Thorburn *et al.*, *Astrophys. J.* **584**, 339–356 (2003).
10. D. Milisavljevic *et al.*, *Astrophys. J.* **782**, L5 (2014).
11. A. G. G. M. Tielens, *The Physics and Chemistry of the Interstellar Medium* (Cambridge Univ. Press, Cambridge, 2005).
12. G. Kordopatis *et al.*, *Astron. J.* **146**, 134 (2013).
13. D. J. Eisenstein *et al.*, *Astron. J.* **142**, 72 (2011).
14. G. Gilmore *et al.*, *Messenger* **147**, 25–31 (2012).
15. J. H. J. de Bruijne, *Astrophys. Space Sci.* **341**, 31–41 (2012).
16. K. C. Freeman, *Galactic Archaeology: Near-Field Cosmology and the Formation of the Milky Way*, W. Aoki, M. Ishigaki, T. Suda, T. Tsujimoto, N. Arimoto, Eds. (2012), vol. 458 of *Astronomical Society of the Pacific Conference Series*, p. 393.
17. L.-C. Deng *et al.*, *Res. Astron. Astrophys.* **12**, 735–754 (2012).
18. T. P. Snow Jr., D. G. York, D. E. Welty, *Astron. J.* **82**, 113 (1977).
19. J. T. van Loon *et al.*, *Astron. Astrophys.* **550**, A108 (2013).
20. S. D. Friedman *et al.*, *Astrophys. J.* **727**, 33 (2011).
21. J. Kos, T. Zwitter, *Astrophys. J.* **774**, 72 (2013).
22. J. Kos *et al.*, *Astrophys. J.* **778**, 86 (2013).
23. H.-C. Chen *et al.*, *Astron. Astrophys.* **550**, A62 (2013).
24. J. Binney *et al.*, *Mon. Not. R. Astron. Soc.* **437**, 351–370 (2014).
25. D. J. Schlegel, D. P. Finkbeiner, M. Davis, *Astrophys. J.* **500**, 525–553 (1998).
26. Supplementary materials are available on *Science* Online.
27. D. B. Sanders, P. M. Solomon, N. Z. Scoville, *Astrophys. J.* **276**, 182 (1984).
28. J. G. A. Wouterloot, J. Brand, W. B. Burton, K. K. Kwee, *Astron. Astrophys.* **230**, 21 (1990).
29. K. R. Sembach, A. C. Danks, *Astron. Astrophys.* **289**, 539 (1994).
30. J. M. Dickey, F. J. Lockman, *Annu. Rev. Astron. Astrophys.* **28**, 215–259 (1990).
31. S. Sharma, J. Bland-Hawthorn, K. V. Johnston, J. Binney, *Astrophys. J.* **730**, 3 (2011).
32. U. Munari *et al.*, *Astron. Astrophys.* **488**, 969–973 (2008).
33. G. A. Gontcharov, *Astron. Lett.* **36**, 584–595 (2010).
34. S. A. Khoperskov, Y. A. Shchekinov, Transport of charged dust grains into the galactic halo (2014); http://arxiv.org/abs/1403.7075 .
35. J. E. G. Peek, Ultraviolet extinction at high galactic latitudes II: The ultraviolet extinction function (2013); http://arxiv.org/abs/1311.2941.



## ACKNOWLEDGMENTS

We are grateful to the anonymous referees for valuable advice on the discussion of possible DIB origins. J.K. and T.Z. thank A. F. Kodre for a stimulating discussion of the topic. Funding for RAVE has been provided by the Anglo-Australian Observatory; the Leibniz-Institut für Astrophysik Potsdam; the Australian National University; the Australian Research Council; the French National Research Agency; the German Research Foundation (SFB 881); the Istituto Nazionale di Astrofisica at Padova; The Johns Hopkins University; the U.S. National Science Foundation (AST-0908326); the W. M. Keck foundation; the Macquarie University; the Netherlands Research School for Astronomy; the Natural Sciences and Engineering Research Council of Canada; the Slovenian Research Agency; Center of Excellence Space.si; the Swiss National Science Foundation; the Science and Technology Facilities Council of the UK; Opticon; Strasbourg Observatory; European Research Council; and the Universities of Groningen, Heidelberg, and Sydney. The RAVE Web site is at www.rave-survey.org.


## SUPPLEMENTARY MATERIALS

www.sciencemag.org/content/345/6198/791/suppl/DC1
Materials and Methods
Supplementary Text
Figs. S1 to S3
References

10 March 2014; accepted 19 June 2014
10.1126/science.1253171

ROBOTICS

# Programmable self-assembly in a thousand-robot swarm

**Michael Rubenstein,* Alejandro Cornejo, Radhika Nagpal**

**Self-assembly enables nature to build complex forms, from multicellular organisms to complex animal structures such as flocks of birds, through the interaction of vast numbers of limited and unreliable individuals. Creating this ability in engineered systems poses challenges in the design of both algorithms and physical systems that can operate at such scales. We report a system that demonstrates programmable self-assembly of complex two-dimensional shapes with a thousand-robot swarm. This was enabled by creating autonomous robots designed to operate in large groups and to cooperate through local interactions and by developing a collective algorithm for shape formation that is highly robust to the variability and error characteristic of large-scale decentralized systems. This work advances the aim of creating artificial swarms with the capabilities of natural ones.**

In nature, groups of thousands, millions, or trillions of individual elements can self-assemble into a wide variety of forms, purely through local interactions. Examples can be found across a wide range of physical scales and systems: at the molecular scale with self-assembly of crystals or rotary motors of bacterial flagella (*1*, *2*), at the cellular scale with the development of multicellular organisms (*3*, *4*), and at the colony level with ants creating structures such as rafts, chains, and nests (bivouacs) using only their interconnected bodies as building material (*5*, *6*). Through collective shape formation, a group can dramatically change how it interacts with its environment. For example, the evolution of multicellular body plans enabled organisms to rapidly fill many ecological niches (*7*), and self-assembly of bridges and bivouacs allows army ant colonies to traverse difficult terrain while providing security and environmental regulation for the queen and brood (*5*). These examples of collective intelligence are fascinating to scientists across disciplines, as much of the global complexity arises from interactions among individuals that are myopic, sensing and interacting at scales many orders of magnitude smaller than the phenomenon itself.

In the field of robotics, researchers use inspiration from collective intelligence in nature to create artificial systems with capabilities observed in natural swarms. Researchers have designed tiny robots, inspired by bees and ants, that are envisioned to work together in large groups, even assembling together to cross difficult terrains (*8*–*10*). Similarly, using inspiration from multicellular development, several groups have

School of Engineering and Applied Sciences and Wyss Institute for Biologically Inspired Engineering, Harvard University, Cambridge, MA 02138, USA.
***Corresponding author. E-mail: mrubenst@seas.harvard.edu**

Science

# Pseudo–three-dimensional maps of the diffuse interstellar band at 862 nm

Janez Kos, Tomaz Zwitter, Rosemary Wyse, Olivier Bienaymé, James Binney, Joss Bland-Hawthorn, Kenneth Freeman, Brad K. Gibson, Gerry Gilmore, Eva K. Grebel, Amina Helmi, Georges Kordopatis, Ulisse Munari, Julio Navarro, Quentin Parker, Warren A. Reid, George Seabroke, Sanjib Sharma, Arnaud Siebert, Alessandro Siviero, Matthias Steinmetz, Fred G. Watson and Mary E. K. Williams

*Science* **345** (6198), 791-795.
DOI: 10.1126/science.1253171

**Clues to a mystery with RAVE results**

An unknown interloper systematically picks off light from galactic sources, snatching at specific wavelengths ranging from the ultraviolet to the infrared. The cause of what astronomers term diffuse interstellar bands (DIBs) still evades identification. Kos *et al.* combined nearly 500,000 stellar spectra from the RAVE survey to make a telling map that may clue us in further. This pseudo–three-dimensional map shows the distribution of the carrier that absorbs light at 862 nm, and it closely follows a separate map of interstellar dust, but with a significantly larger scale height in the Galactic plane. Though this is only one DIB of many, this analysis sets a path for the future study of others.

*Science*, this issue p. 791